separations

MDPI

Article

Inserting an Additional Vortex Finder to Improve the Performance of Cyclones in Series

Weihong He [1], Jingxuan Yang [1,*] and Guogang Sun [2,3,*]

[1] College of Chemistry and Chemical Engineering, Taiyuan University of Technology, Taiyuan 030024, China; heweihongsl@163.com
[2] State Key Laboratory of Heavy Oil Processing, China University of Petroleum, Beijing 102249, China
[3] Beijing Key Laboratory of Process Fluid Filtration and Separation, Beijing 102249, China
* Correspondence: yangjingxuan@tyut.edu.cn (J.Y.); ggsunbj@163.com (G.S.)

Abstract: Multiple cyclones working in series are sufficient for heavy separation tasks at the cost of significant energy consumption. The majority of researchers conducting optimization studies on multiple cyclones have attempted to find the best possible compromise between pressure drop and collection efficiency by optimizing the geometry of the cyclones. In a departure from this approach, we report a novel design. Using the proposed method, exit gas is divided into dirty and clean gas by inserting a secondary vortex finder (SVF) into the primary vortex finder (PVF) of the previous cyclone. The dirty gas flows into the succeeding cyclone, whereas the clean gas passes over the succeeding cyclone and directly flows into the device farther behind. Methodologically, the separation performance was tested experimentally, and computational fluid dynamics (CFD) simulations were employed. The Reynolds Stress Model (RSM) for turbulence and the Discrete Phase Model (DPM) were used to simulate the turbulent two-phase flow within the gas–solid separator, capturing the three-dimensional, transient, and turbulent characteristics of the flow. Our performance test results showed that the new series configuration clearly reduces energy consumption while not hindering overall efficiency. The CFD simulation was used to optimize the SVF's diameter and length. The results indicated that having an SVF with optimal dimensions significantly enhances the vortex flow in the separation space and thus improves the efficiency of the previous cyclone. In addition, an equation was established that describes the volume of gas flowing into a succeeding cyclone.

Keywords: cyclones in series; additional vortex finder; efficiency; pressure drop

check for updates

Academic Editor: Yundong Wang

Received: 4 February 2025
Revised: 23 February 2025
Accepted: 27 February 2025
Published: 3 March 2025

Citation: He, W.; Yang, J.; Sun, G. Inserting an Additional Vortex Finder to Improve the Performance of Cyclones in Series. *Separations* **2025**, *12*, 60. https://doi.org/10.3390/separations12030060

Copyright: © 2025 by the authors. Licensee MDPI, Basel, Switzerland. This article is an open access article distributed under the terms and conditions of the Creative Commons Attribution (CC BY) license (https://creativecommons.org/licenses/by/4.0/).

1. Introduction

A cyclone separator is a device that uses centrifugal force to separate solid particles or liquid droplets. Owing to their simple construction and operation, ease of maintenance, and flexibility, cyclone separators offer favorable reliability and cost, particularly under high-temperature conditions [1]. In the petroleum refining and petrochemical industries, cyclone separators are employed to recover expensive catalysts. In the photovoltaic industry, they are used to recycle unreacted silicon materials for reuse. In the coal-fired power generation industry, cyclone separators aid in the control of pollutant emissions. In CCUS (Carbon Capture, Utilization, and Storage) technologies, cyclone separators are utilized for the efficient separation and recovery of solid particles or liquid droplets from gases, thereby reducing carbon dioxide emissions and those of other greenhouse gases [2–4]. To enhance the performance of a cyclone, the majority of researchers thus far have focused on optimizing the geometrical and operational factors of a single cyclone [5–11]. However,

there are many situations wherein a single cyclone is inadequate for a separation task; for instance, under a high solid concentration loaded in an air environment [12]. In such situations, several cyclones usually operate in series [13–15]. Such an arrangement not only induces higher separation efficiency but also results in a greater pressure drop, which directly increases operational costs. Therefore, it is necessary to find a satisfactory balance between separation efficiency and pressure drop.

As reported by Whitelock and Buser [13], compared with a single cyclone configuration, two cyclones operating in series can substantially improve efficiency with an acceptable increase in pressure drop. However, the addition of a succeeding cyclone in the series configuration only slightly improves efficiency but with a concurrent significant increase in pressure drop. A series configuration using two-stage separation provides a better balance. Many researchers agree on this point and have focused on the performance improvement of two-stage cyclones operating in series. McCallion [16] designed novel two-stage cyclones operating in series, including a large cyclone in the first stage and two small cyclones in the second stage, thereby successfully replacing the three-stage cyclones used in series in acrylonitrile reactors for catalyst recycling. According to Chen [17], decreasing the cyclone diameter and increasing the amount used in the second stage contributes to the improved performance of McCallion's design. Chen [17] tested similar two-stage cyclones in series, including two small cyclones in the first stage and a large cyclone in the second stage. Their results showed a level of performance close to that of McCallion's design, and both designs achieved a better level of performance than the three-stage cyclones applied in series. To reduce the number of cyclones and save space in an acrylonitrile reactor, Chen [18] included two cyclones in a two-stage cyclone design used in series, in which a PV-E type cyclone is applied as a second collector to a normal cyclone used as the first collector. A PV-E type cyclone includes a novel vortex finder [19,20], resulting in a 2–3% improvement in separation efficiency. Gillum et al. [14] found that a 1D3D secondary cyclone contributes to better separation efficiency than a 2D2D secondary cyclone when both are connected to a 2D2D primary cyclone. In this case, a 2D2D cyclone refers to both the body and cone length being twice the diameter of the body. Similarly, a 1D3D cyclone means that the body length equals the body diameter; in comparison, the cone length is triple the body diameter. In addition to their investigation, Luciano et al. [21] set up optimization procedures based on computational fluid dynamics to minimize the pressure drop and maximize the efficiency of three cyclones applied in series. Each cyclone separator in the series configuration was designed with an optimized geometric structure.

It should be noted that the authors of the aforementioned studies focused on optimizing the geometry of an individual cyclone and decreasing the number of cyclones to improve the series configuration. Because dirty gas passes through multiple cyclones in a step-by-step manner, there is little beneficial interaction in the collection between the previous and succeeding cyclones. Increasing the efficiency of the previous cyclone generally leads to more difficulty regarding the capture of particles in the succeeding cyclone owing to the decreased dust loading. In contrast, the improved succeeding cyclone has little effect on the previous cyclone. A recirculation cyclone developed by Salcedo et al. [22–24] provided a suitable solution to this problem. Dirty gas first passes through a reverse flow cyclone and then flows into a straight-through cyclone with or without an electrostatic field. The clean gas at the center part of the secondary cyclone flows out while the particles concentrate on the wall. Instead of being collected, they mix with the fresh dirty gas and flow into the first cyclone again for collection. The recirculation of particles in the secondary cyclone improves particle agglomeration, which is beneficial with regard to particle capture, particularly for small-scale particles. Fu et al. reported another beneficial interaction between the previous and succeeding cyclones [25,26]. A suitable style directly

connecting the dust outlet of the previous cyclone and the inlet of the succeeding cyclone prompted the smaller particles to enter the succeeding cyclone from the radially outer side and axially lower side at the rectangular inlet. As a result, the efficiency of the succeeding cyclone significantly improved.

In this study, we investigate another method regarding the beneficial interaction between the previous and succeeding cyclones. Rather than achieving an improvement in efficiency, similar to Salcedo's approach, the proposed design reduces the pressure drop without decreasing the overall separation efficiency, thereby providing another method to obtain a satisfactory balance between separation efficiency and pressure drop in cyclones used in series.

2. Design and Method

2.1. Design

A strong gas-swirling motion is applied in a cyclone for particle collection. In general, a strong gas swirl is also present in a vortex finder. Based on measurements obtained by Hu et al. [27], the maximum tangential velocity of gas in a vortex finder is approximately 94% of that in a cyclone body. As a result, the escaped particles are centrifuged at the wall in the vortex finder and the gas in the center part is much cleaner, which is similar to that demonstrated in a cyclone body. In the normal series configuration shown in Figure 1a, the dirty gas near the wall and the clean gas in the center ultimately mix together and flow into the succeeding cyclone. To utilize the vortex in the vortex finder, Sun et al. [28] proposed a new design using multiple series of cyclones, where a secondary vortex finder, shown in Figure 1b, is inserted into the primary vortex finder to separate the two types of gases. The dirty gas flows into the succeeding cyclone, whereas the clean gas passes over the succeeding cyclone and flows directly into the device farther behind. Theoretically, the dust loading of gas into the succeeding cyclone in our design is higher than that in a normal series configuration, which contributes to particle capture. In addition, because not all of the gas flows into the succeeding cyclone, our design consumes less gas energy than a normal series configuration.

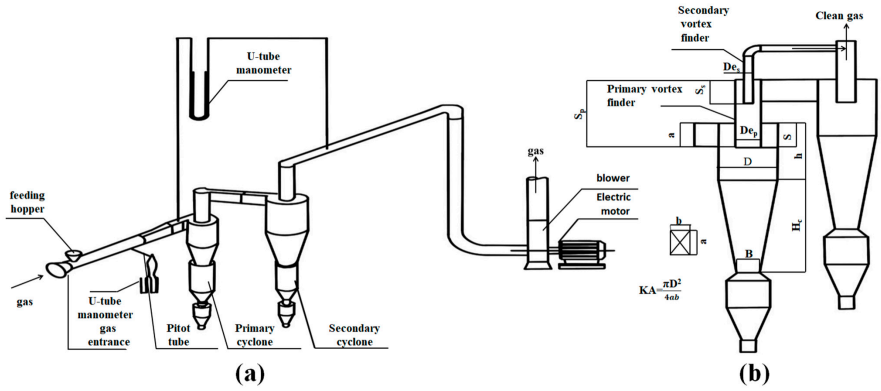


Figure 1. Schematic illustration of the experimental equipment: (**a**) the experimental apparatus and (**b**) the geometries of two-stage cyclones [28].

2.2. Experiment

The experimental apparatus and features of two-stage cyclones used in series are shown in Figure 1. A fan blower at the end of the flow installation was used to enable air of normal temperature and pressure to enter the system. Behind the air entrance, a hopper was applied to feed in the test dust. In the experiment, 800-mesh talc powder (ρ = 2700 kg/m^3) with a particle size distribution spanning 0.2–80 μm was utilized, exhibiting a median particle size of 8.04 μm. A total of 1 kg of dust was fed into the system during each

experiment, with the dust load maintained at approximately 10 g of dust/m^3 gas by controlling the time of the feeding. The mathematical relationship between concentration C_i and feeding time t_i is governed by the following coupled Equations (1) and (2):

$$t_i = \frac{w}{C_i \times Q_{in}} \tag{1}$$

$$C_i = \frac{w}{t_i \times Q_{in}} \tag{2}$$

In the formula, *W* represents the amount of material added each time, in grams (g); *Ci* is the concentration of the added material, in grams per cubic meter (g/m^3); and *Q*in is the gas volumetric flow rate entering the separator, in cubic meters per second (m^3/s). The gas volumetric flow is the rate of the product in the inlet area and the inlet gas velocity *V*in.

The dust-laden air passed through the multiple series cyclones that removed most of the dust. The dust was collected in the hopper underneath each cyclone and weighed to measure the separation efficiency. The remaining dust was captured using the succeeding filter. The separation efficiency η is mathematically defined by Equation (3).

$$\eta = \frac{m}{M} \tag{3}$$

where *M* represents the total mass of the added powder (g) and *m* denotes the mass of the collected powder (g).

A Pitot tube was used to measure the gas speed. The inlet gas velocity was varied in three steps within a range of 17 to 21 m/s. The measurement principle is based on Bernoulli's equation, and the measurement formula is shown in Equation (4).

$$V = \sqrt{2\frac{\delta P}{\rho}} \tag{4}$$

where *V* represents the velocity of the gas (m/s); δP denotes the difference between the total pressure and the static pressure (Pa); and ρ represents the density of the gas (kg/m^3).

The pressure drop measurement in the cyclone separators using U-type manometers operates on the principle of hydrostatic equilibrium and pressure transmission. When differential pressure (ΔP) acts on the U-tube, the working fluid (typically water or mercury) forms a measurable height difference (*h*) between the two columns, and is expressed as follows:

$$\Delta P = \rho g h \tag{5}$$

where ρ represents the fluid density (kg/m^3); *g* denotes the gravitational acceleration (9.81 m/s^2); and *h* represents the liquid column height difference (m).

2.3. Computational Fluid Dynamics Simulation

2.3.1. The CFD Method

The commercial CFD software ANSYS Fluent 15.1 was employed to investigate flow patterns in the two series-configured cyclone separators. In light of the anisotropic strong swirling flow characteristics within the cyclones, the gas phase was mathematically described using Navier–Stokes equations, with turbulence closure achieved through the Reynolds Stress Model (RSM). The governing equations are expressed as follows:

(1) Continuity equation

$$\frac{\partial \rho}{\partial t} + \frac{\partial}{\partial x_i}(\rho \overline{u}_i) = 0 \tag{6}$$

(2) Momentum equation

$$\frac{\partial}{\partial t}(\rho \overline{u}_i) + \frac{\partial}{\partial x_j}\left(\rho \overline{u}_i \overline{u}_j\right) = -\frac{\partial \overline{p}}{\partial x_i} + \frac{\partial}{\partial x_j}\left(\mu \frac{\partial \overline{u}_i}{\partial x_j} - \rho \overline{u_i' u_j'}\right) \tag{7}$$

In the equations, u_i represents the instantaneous velocity components, $\overline{u}_i$ represents the mean velocity components, $u' = u_i - \overline{u}_i$ represents the fluctuating velocity components, x_i represents the spatial coordinates, $\overline{u_i'u_j'}$ represents the Reynolds stress components, and the subscripts i, j, k = 1, 2, 3. $\overline{p}$ represents the mean pressure, ρ represents the fluid density, μ represents the dynamic viscosity of the fluid, and t represents time.

(3) Reynolds Stress Transport Equation

$$\frac{\partial}{\partial t}\left(\rho\overline{u_i'u_j'}\right) + \frac{\partial}{\partial x_k}\left(\rho u_k\overline{u_i'u_j'}\right) = D_{ij} + P_{ij} + G_{ij} + \Phi_{ij} - \varepsilon_{ij} + F_{ij} \quad (8)$$

In the equation, D_{ij} represents the diffusion term, P_{ij} represents the production term due to shear stress, G_{ij} represents the production term due to buoyancy, Φ_{ij} represents the stress–strain term, ε_{ij} represents the viscous dissipation term, and F_{ij} represents the term due to system rotation.

In solving the governing equations, pressure–velocity coupling was addressed using the SIMPLEC (Semi-Implicit Method for Pressure-Linked Equations Consistent) algorithm. The pressure gradient term was addressed with the PRESTO (Pressure Staggering Option) method, with all of the convective terms being discretized using the QUICK (Quadratic Upwind Interpolation for Convective Kinematics) scheme. Additionally, a transient simulation was conducted with a time step of 0.0002 s [29].

2.3.2. Boundary Conditions

With the exception of the diameter and length of the SVF, the dimensions of the separator model remained identical to those of the experimental equipment. To investigate the effects of the SVF on the flow pattern inside the primary cyclone, the dimensionless diameter and length of the SVF were varied in several steps, as shown in Table 1.

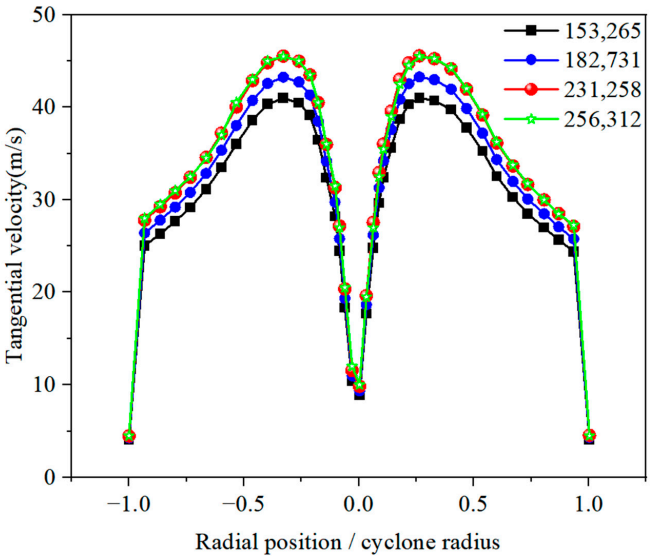
The velocity inlet was used as the boundary condition. The inlet gas velocity was set to 21 or 15 m/s, and its direction was normalized to the inlet boundary. The hydraulic diameter and turbulent intensity are shown in Table 1. The boundary condition at the cyclone outlet is prescribed as a fully developed pipe flow and treated as an "outflow" in FLUENT. With the exception of the inlet and outlet, all other boundaries were treated as a wall. A no-slip condition was assumed at the wall. The grid nodes near the wall were approximated and treated using the standard FLUENT wall functions.

Table 1. The geometric dimensions of cyclones and boundary conditions thereof during CFD simulation.

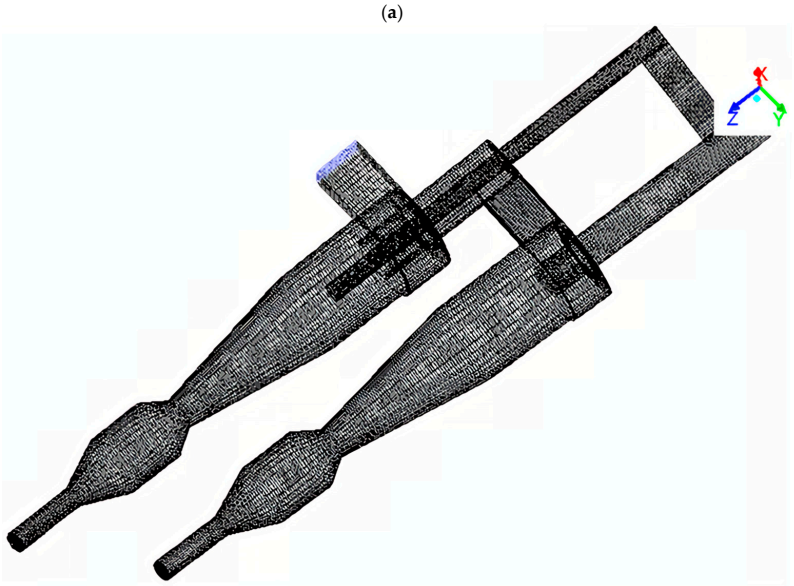
Terms	The Primary Cyclone					The Secondary Cyclone
	Experiment			Simulation		
D (mm)	300			300		300
KA	5.5			5.5		7.5
De_p/D	0.53			0.53		0.4
S/D	0.59			0.59		0.49
H/D	3.4			3.4		3.4
h/D	1.4			1.4		1.4
B/D	0.4			0.4		0.4
De_s/De_p	0	0.4		0 0.5	0.25 0.7	0.4 ---
S_s/S_p	0	0.65		0 1	0.27 1.35	0.65 ---
Inlet velocity (m/s)	17	19	21	15	21	---
Hydraulic diameter at the inlet (mm)	---			113.7	113.7	---
Turbulent intensity at the inlet	---			3.77%	3.62%	---

2.3.3. Mesh Independence and Model Validation

The simulation employed hexahedral meshes. To verify mesh independence, the structure with a cylinder diameter of D = 300 mm was selected, and four different mesh counts were used: 153,265, 182,731, 231,258, and 256,312. Figure 2a,b shows the tangential velocity and the meshing model, respectively. It is evident that once the mesh count reaches 231,258, the tangential velocity no longer varies with further increases in mesh count. While higher mesh counts lead to longer computation times and greater difficulty in convergence, a balance between computational efficiency and accuracy is necessary. Therefore, the final mesh count of 231,258 was chosen. To validate the simulation method, the tangential velocity within the cyclone separator measured experimentally by Hu et al. [30] was used as a reference. The simulated tangential velocity obtained using the method presented in this study under the same conditions was compared with the experimental data, as shown in Figure 2c. The results indicate that the simulation data are in good agreement with the experimental measurements, thereby demonstrating the reliability of the simulation approach.

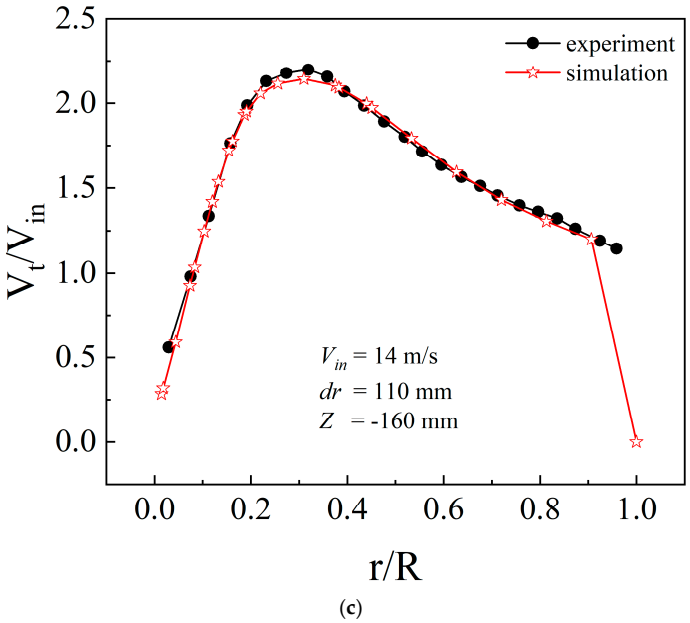


(**a**)



(**b**)

Figure 2. *Cont.*



(**c**)

Figure 2. (**a**) Mesh independence verification; (**b**) mesh model; (**c**) validation of the CFD simulation method.

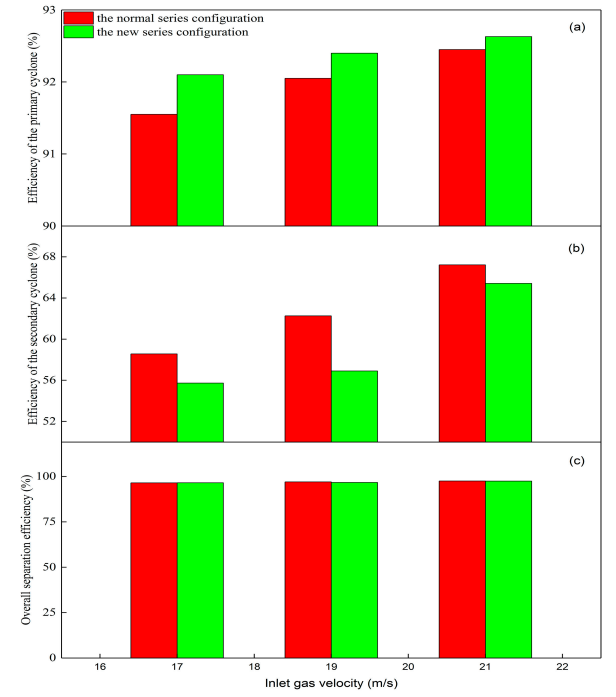
3. Results and Discussion

3.1. Experimental Separation Efficiency and Pressure Drop

The performance results of the novel and normal two-stage cyclones used in series are shown in Figure 3. As evidenced, the ability to decrease the pressure drop is the advantage of the new series configuration. Under the new configuration, when the inlet gas velocity is 17 m/s, the pressure drop is reduced by 33% compared to the conventional two-stage cyclone separator. When the inlet velocity is 19 m/s, the pressure drop is reduced by 33.8% compared to the conventional two-stage cyclone separator. When the inlet velocity reaches 21 m/s, the pressure drop is reduced by 36.8%. Therefore, it can be concluded that the higher the inlet velocity, the greater the energy-saving effect that can be achieved. When comparing the overall separation efficiency of the two configurations, it can be seen that the conventional series-connected two-stage cyclone separator exhibits a marginally higher separation efficiency than the novel series-connected two-stage cyclone separator. Specifically, the maximum difference in separation efficiency is observed at a gas velocity of 19 m/s, where the maximum difference is less than 0.3%. As an interesting phenomenon, the efficiency of the primary cyclone in the new series configuration was slightly higher than that in the normal configuration, whereas the efficiency of the secondary cyclone was much lower. The decrease in overall efficiency in the new configuration is thus derived from the reduction in the efficiency of the secondary cyclone. Therefore, the secondary cyclone used in the new series configuration does not have the best design. In the two experimental configurations, the dimensions of the secondary cyclone were identical. Because only some of the gas flowed into the secondary cyclone in the new configuration, the inlet gas velocity of the secondary cyclone was much lower than that in the normal configuration, which resulted in a reduction in separation efficiency. Therefore, it can be hypothesized that reducing the dimensions, similar to the method followed in the study by McCallion [16], and increasing the inlet gas velocity of the secondary cyclone might improve the overall separation efficiency of the new series configuration.

In previous works, Ray et al. [31,32] and Souza [33] described a device called a post-cyclone used to collect the escaped particles in the vortex finder and thereby increasing efficiency. Although a post-cyclone also utilizes the swirl present in the vortex finder,

similar to our design, there is still a significant difference between the two approaches. In the new configuration, the primary cyclone does not collect the particles in the vortex finder. The improvement in efficiency is derived from the enhanced swirl in the separation space, which captures more particles. Evidence of this change was demonstrated through a CFD simulation. Concurrently, the succeeding cyclone also benefited because the dust load of the gas was improved, which contributed to the capture of small particles. In contrast, the post-cyclone consumes approximately 10% of the total pressure drop over the cyclone; in comparison, the new configuration reduces the total pressure drop over the cyclones in series by 33%. Kępa [34] reported the results of a CFD analysis of the flow inside a cyclone using a doubled vortex finder, which is similar to our design. However, in their CFD analysis, they found a reduction in efficiency in a cyclone with a doubled vortex finder. The evident gap between the two investigations may be due to the different dimensions of the vortex finder applied. More details in this regard were demonstrated through CFD analysis.



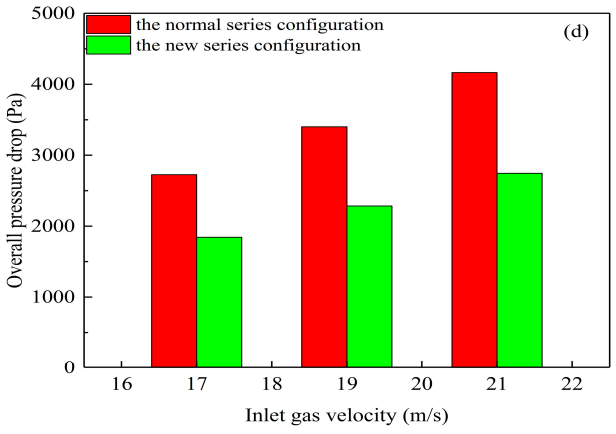


Figure 3. The experimental performance of normal and new series configurations: (**a**) separation efficiencies of the primary cyclone in both configurations; (**b**) separation efficiencies of the secondary cyclone in both configurations; (**c**) overall separation efficiency in both configurations; (**d**) overall pressure drop in both configurations.

3.2. Effects of the Secondary Vortex Finder on the Flow Pattern in a Cyclone

Although the results of the experiment demonstrated the advantages of the new series configuration, a CFD simulation was necessary to obtain more information on the flow pattern in order to optimize the dimensions of the series configuration, particularly the diameter and length of the secondary vortex finder (SVF) in the primary cyclone.

3.2.1. Tangential Velocity

The effects of the dimensions of the SVF on the tangential velocity in the separation space of the primary cyclone are shown in Figure 4. It was observed that the maximum tangential velocity in the experimental cyclone with the SVF (represented as a solid upward triangle in Figure 4a) was higher than that in the normal cyclone. As is widely recognized, the tangential velocity is closely related to the centrifugal force, which allows the particles to be captured. Therefore, the improved efficiency of the primary cyclone in the new series configuration can be attributed to the enhanced tangential velocity. In addition, Figure 4a provides more details on the effects of the SVF's length on the tangential velocity. It is clear that extending the length of the SVF improves the tangential velocity. However, the improvement stagnates when the gas entrances of both the SVF and PVF are located at the same axial position in the cyclone. Therefore, to enhance the efficiency of the primary cyclone, the SVF entrance should be positioned lower than the PVF entrance, as shown in Figure 4b.

As shown in Figure 4b, it is also significant that the diameter of the SVF (De_s) ranges from 0.4 to 0.5 that of the PVF (De_p), which is optimum because such a diameter yields the maximum improvement in the tangential velocity in the separation space of the primary cyclone. Decreasing or increasing the diameter of the SVF reduces the improvement in the tangential velocity. From the results, it is evident that when De_s/De_p is increased to 0.7 or reduced to 0.25, the maximum tangential velocity almost equals that in the normal cyclone. Alternatively, a clear trend regarding the increasing tangential velocity with a decrease in the diameter of the vortex finder was observed inside a normal cyclone with only a single vortex finder. Although these differences are difficult to explain, we still find them plausible because they correspond to the results cited in other studies. Based on the analysis results, De_s/De_p = 0.7 of the SFV results in 66% gas extraction through the PVF and a profile of tangential velocity extremely similar to that in a normal cyclone. Thus, enlarging De_s/De_p further does not change the profile of the tangential velocity. Kępa [35] analyzed the tangential velocity profiles in cyclones with 20%, 40%, and 57% gas extraction through the PVF, corresponding to $De_s/De_p > 0.7$, and found little difference among them, in agreement with the results of the present study. In addition, Kępa [35] found that none of these values were advantageous in terms of efficiency when compared with a normal cyclone. Based on the results of the present study, an overly high bleed flow provides one possible explanation.

However, the boundary between the inner and outer vortexes is usually close to the center of the cyclone when the diameter of the vortex finder decreases inside a normal cyclone. In the new configuration, a similar phenomenon could also be observed when the diameter of the SVF ranged from 0.7 to 0.4 De_p. However, when the diameter of the SVF was reduced to 0.25 De_p, the profile of the tangential velocity was quite similar to that in a normal cyclone. The results indicate that the SVF contributed to the enhancement of the vortex in the separation space when the dimensionless diameter ranged from 0.4 to 0.5 De_p. When the diameter was too small or too large, the effect of the SVF on the profile of the tangential velocity in the separation space was not clear.

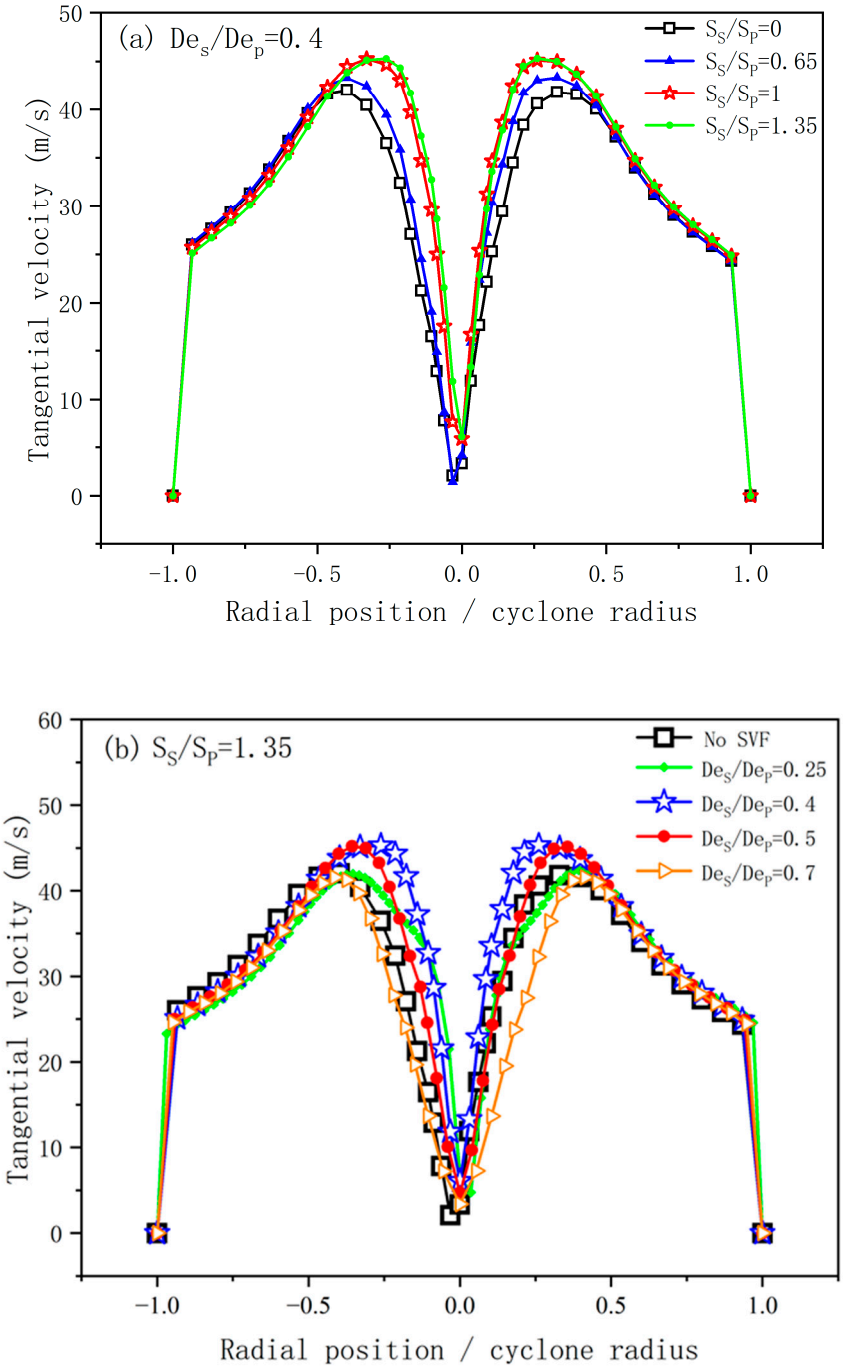


Figure 4. The effect of the secondary vortex finder dimensions on tangential velocity: (**a**) length and (**b**) diameter.

3.2.2. Gas Volume Through the PVF

As detailed above, it is necessary to determine how much gas flows through the PVF in order to optimize the dimensions of the secondary cyclone. Figure 5 shows the results based on a CFD simulation. It can be observed that extending the length of the SVF from S_2 / S_1 = 0.27 to S_2 / S_1 = 1.35 resulted in a 3% improvement in the gas volume flowing into the secondary cyclone, as indicated in Figure 5a. When the gas entrances of both the SVF and PVF are located at the same axial position in the cyclone, the gas volume reaches the maximum value. In addition, a further extension of the SVF does not result in any changes.

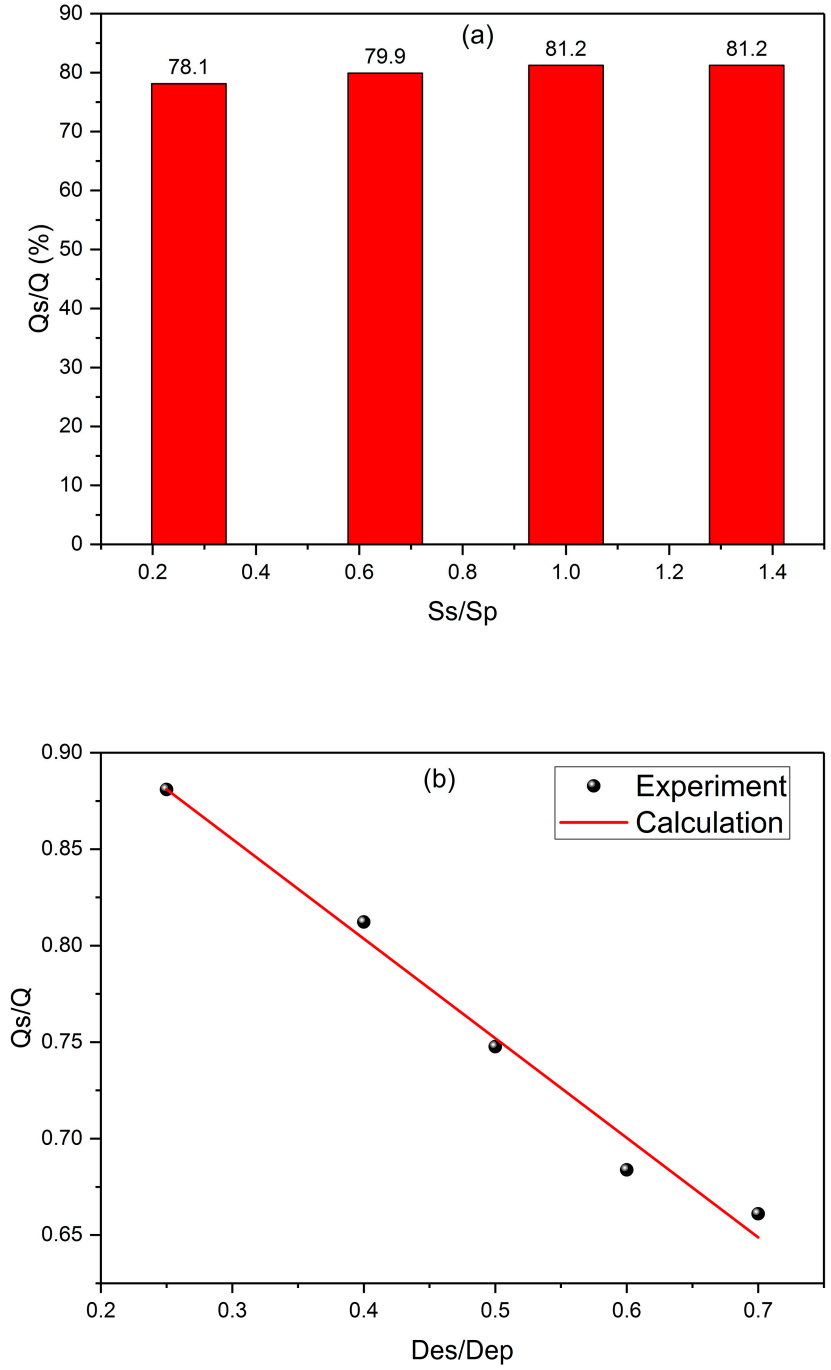


Figure 5. The effect of secondary vortex finder dimensions on the gas volume flowed into the secondary cyclone: (**a**) length and (**b**) diameter.

Compared with the length, the diameter has a more significant effect on the gas distribution. Figure 5b shows a clear trend regarding the decreasing gas volume flowing into the secondary cyclone with the enlargement of the SVF. This trend can be described as follows:

$$\frac{Q_s}{Q} = 1.010 - 0.516\frac{De_s}{De_p} \quad (9)$$

where Q_s is the gas volume flowing into the secondary cyclone and Q is the gas volume flowing into the primary cyclone. Although the inlet gas velocity is closely related to Q, the CFD analysis results indicate that it has little effect on the gas distribution. It should be noted that Equation (1) is based on a primary cyclone with an SVF of S_2/S_1 = 1.35. If

the SVF entrance is not positioned lower than the PVF entrance, there should be a 1–3% increase in Q_s/Q.

4. Conclusions

In the present work, we present a new configuration of multiple cyclones working in series. Inserting an additional vortex finder into the original finder can allow the inner vortex flow to divide the exit gas into two forms: one dirty and the other clean. The dirty gas flows into the succeeding cyclone, whereas the clean gas passes over the succeeding cyclone and directly flows into the device further behind. The results of a performance experiment indicated that the new configuration consumes less gas energy without hindering overall efficiency. In addition, the efficiency of the primary cyclone increases because the SVF contributes to the enhancement of the vortex in the separation space. When De_s/De_p ranges from 0.4 to 0.5, the positive effect is significant. When the diameter of the SVF is too large or too small, the beneficial flow pattern is no longer observed. To utilize this positive effect and improve efficiency, the SVF should be designed as follows: (1) De_s/De_p should vary from 0.4 to 0.5 and (2) the SVF entrance should be positioned lower than the PVF entrance. In addition, an equation used to calculate the gas distribution between the two vortex finders was proposed to optimize the succeeding cyclone.

Author Contributions: Conceptualization, G.S.; methodology, J.Y. and W.H.; software, W.H.; validation, J.Y.; resources, J.Y.; data curation, W.H.; writing—original draft preparation, W.H.; writing—review and editing, G.S. and J.Y.; supervision, G.S. and J.Y. All authors have read and agreed to the published version of the manuscript.

Funding: This research was supported by the Fundamental Research Program of Shanxi Province (grant No. 202203021211164). The authors also gratefully acknowledge the support from the National Natural Science Foundation of China (grant No. 22378285).

Data Availability Statement: The original contributions presented in this study are included in the article.

Conflicts of Interest: The authors declare no conflict of interest.

References

1. Zhang, J.; You, C.F.; Qi, H.Y.; Hou, B.; Chen, C.H.; Xu, X.C. Effect of Operating Parameters and Reactor Structure on Moderate Temperature Dry Desulfurization. *Environ. Sci. Technol.* **2006**, *40*, 4300–4305. [CrossRef] [PubMed]
2. Amiri, M.; Ziółkowski, P.; Mikielewicz, J.; Klugmann, M.; Mikielewicz, D. Analysis of cyclone separator solutions depending on spray ejector condenser conditions. *Appl. Therm. Eng.* **2024**, *257*, 124235. [CrossRef]
3. Amiri, M.; Mikielewicz, J.; Mikielewicz, D. CO_2 capture using steam ejector condenser under electro hydrodynamic actuator with non-condensable gas and cyclone separator: A numerical study. *Sep. Purif. Technol.* **2024**, *329*, 125236. [CrossRef]
4. Amiri, M.; Mikielewicz, J.; Ziółkowski, P.; Mikielewicz, D. Optimizing CO_2 Purification in a Negative CO_2 Emission Power Plant. *Chem. Eng. Technol.* **2024**, *47*, e202300568. [CrossRef]
5. Wu, K.B.; Liu, G.F.; Weng, J.S. Numerical simulation and experimental study on pressure drop of radial jet cyclone. *Sep. Purif. Technol.* **2016**, *166*, 9–15. [CrossRef]
6. Pei, B.; Yang, L.; Dong, K.; Jiang, Y.; Du, X.; Wang, B. The effect of cross-shaped vortex finder on the performance of cyclone Separator. *Powder Technol.* **2017**, *313*, 135–144. [CrossRef]
7. Misiulia, D.; Andersson, A.G.; Lundström, T.S. Effects of the inlet angle on the collection efficiency of a cyclone with helical-roof inlet. *Powder Technol.* **2017**, *305*, 45–88. [CrossRef]
8. Brar, L.S.; Elsayed, K. Analysis and optimization of multi-inlet gas cyclones using large eddy simulation and artificial neural network. *Powder Technol.* **2017**, *311*, 465–483. [CrossRef]
9. Sun, X.; Kim, S.; Yang, S.D.; Kim, H.S.; Yoon, J.Y. Multi-objective optimization of a Stairmand cyclone separator using response surface methodology and computational fluid dynamics. *Powder Technol.* **2017**, *320*, 51–65. [CrossRef]
10. Sun, X.; Yoon, J.Y. Multi-objective optimization of a gas cyclone separator using genetic algorithm and computational fluid dynamics. *Powder Technol.* **2017**, *325*, 347–360. [CrossRef]

11. Wasilewski, M.; Brar, L.S. Optimization of the geometry of cyclone separators used in clinker burning process: A case study. *Powder Technol.* **2017**, *313*, 293–302. [CrossRef]
12. Hoffmann, A.C.; Stein, L.E. *Gas Cyclones and Swirl Tubes: Principles, Design and Opration*, 2nd ed.; Springer: Berlin/Heidelberg, Germany, 2007.
13. Whitelock, D.P.; Buser, M.D. Multiple series cyclones for high particulate matter concentrations. *Appl. Eng. Agric.* **2007**, *23*, 131–136. [CrossRef]
14. Gillum, M.N.; Hughs, S.E.; Armijo, B.M. Use of secondary cyclones for reducing gin emissions. *Trans. ASABE.* **1982**, *25*, 210–213. [CrossRef]
15. Sun, G.G.; Chen, J.Y.; Shi, M.X. Optimization and applications of reverse-flow cyclones. *China Particuology* **2005**, *3*, 43–46. [CrossRef]
16. Mccallion, J. New separation approach saves catalyst and energy. *Chem. Process.* **1996**, *59*, 73–74.
17. Chen, J.Y.; Shi, M.X. Research on feasible designs of two-stage cyclone separators for acrylonitrile reactors. *Petro-Chem. Equip.* **2001**, *30*, 4–7. (In Chinese)
18. Chen, J.Y.; Shi, M.X. An experimental research on the full-scale cold model of the new two-stage cyclone separator for acrylonitrile reactors. *Chem. Eng. Mach.* **2001**, *28*, 249–254. (In Chinese)
19. Li, Q.; Xu, W.W.; Wang, J.J.; Jin, Y.H. Performance evaluation of a new cyclone separator—Part I experimental results. *Sep. Purif. Technol.* **2015**, *141*, 53–58. [CrossRef]
20. Xu, W.W.; Li, Q.; Wang, J.J.; Jin, Y.H. Performance evaluation of a new cyclone separator—Part II simulation results. *Sep. Purif. Technol.* **2016**, *160*, 112–116. [CrossRef]
21. Luciano, R.D.; Silva, B.L.; Rosa, L.M.; Meier, H.F. Multi-objective optimization of cyclone separators in series based on computational fluid dynamics. *Powder Technol.* **2018**, *325*, 452–466. [CrossRef]
22. Salcedo, R.L.R. Recirculation Cyclones for Dedusting and Dry Gas. Cleaning. Patent WO0141934, 14 June 2001.
23. Salcedo, R.L.R.; Fonseca, A.M.; Chibante, V.G.; Cândido, G. Fine particle capture in biomass boilers with recirculating gas cyclone: Theory and practice. *Powder Technol.* **2007**, *172*, 89–98. [CrossRef]
24. Salcedo, R.L.R. Process of Electrostatic Recirculation for Dedusting and Gas Cleaning and Device. Thereof. Patent WO20088147233, 4 November 2008.
25. Fu, P.B.; Jiang, X.; Ma, L.; Yang, Q.; Bai, Z.S.; Yang, X.J.; Chen, J.Q.; Yuan, W.; Wang, H.L.; Lv, W.J. Enhancement of PM2.5 Cyclone Separation by Droplet Capture and Particle Sorting. *Environ. Sci. Technol.* **2018**, *52*, 11652–11659. [CrossRef] [PubMed]
26. Fu, P.B.; Wang, F.; Yang, X.J.; Ma, L.; Cui, X.; Wang, H.L. Inlet Particle-Sorting Cyclone for the Enhancement of PM2.5Separation. *Environ. Sci. Technol.* **2017**, *51*, 1587–1594. [CrossRef] [PubMed]
27. Hu, L.Y.; Zhou, L.X.; Zhang, J.; Shi, M.X. Studies on strongly swirling flows in the full space of a volute cyclone separator. *AIChE J.* **2005**, *51*, 740–749. [CrossRef]
28. Sun, G.G.; Yang, J.X. Multiple Series Cyclones with Distributary Exhaust Used in Fluid Bed. Patent ZL201110318123.6, 3 June 2015.
29. Yang, J.X.; Sun, G.G.; Gao, C.Z. Effect of the inlet dimensions on the maximum-efficiency cyclone height. *Sep. Purif. Technol.* **2012**, *160*, 112–116. [CrossRef]
30. Hu, L.Y.; Shi, M.X. Three-dimensional time-averaged flow structure in cyclone separator with volute inlet. *J. Chem. Ind. Eng.* **2003**, *54*, 549–556.
31. Ray, M.B.; Luning, P.E.; Hoffmann, A.C.; Maurice, A.P.; Beumer, I.L. Improving the removal efficiency of industrial-scale cyclones for particles smaller than five micrometer. *Int. J. Miner. Process.* **1998**, *53*, 39–47. [CrossRef]
32. Jo, Y.; Tien, C.; Ray, M.B. Development of a post cyclone to improve the efficiency of reverse flow cyclones. *Powder Technol.* **2000**, *113*, 97–108. [CrossRef]
33. Souza, F.J.D.; Salvo, R.D.V.; Martins, D.D. M Simulation of the performance of small cyclone separators through the use of Post Cyclone (PoC) and annular overflow ducts. *Sep. Purif. Technol.* **2015**, *142*, 71–82. [CrossRef]
34. Kępa, A. Division of outlet flow in a cyclone vortex finder-The CFD calculations. *Sep. Purif. Technol.* **2010**, *75*, 127–131. [CrossRef]
35. Kępa, A. CFD investigation of a flow inside a cyclone with additional gas extraction. *Chem. Process Eng.* **2008**, *29*, 1027–1035.

Disclaimer/Publisher's Note: The statements, opinions and data contained in all publications are solely those of the individual author(s) and contributor(s) and not of MDPI and/or the editor(s). MDPI and/or the editor(s) disclaim responsibility for any injury to people or property resulting from any ideas, methods, instructions or products referred to in the content.